AGU PUBLICATIONS

JGR

Journal of Geophysical Research: Space Physics

RESEARCH ARTICLE

10.1002/2015JA022146

This article is a companion to 2015JA022179.

Key Points:
- Connection between electric fields and plasma drifts under prompt penetration electric field
- Anomalous behavior of daytime zonal drift in the absence of any magnetic storm
- Anticorrelation between vertical and zonal drifts during magnetic storms

Correspondence to:
A. M. Santos,
angela.santos@inpe.br;
angelasantos_1@yahoo.com.br

Citation:
Santos, A. M., M. A. Abdu, J. R. Souza, J. H. A. Sobral, and I. S. Batista (2016), Disturbance zonal and vertical plasma drifts in the Peruvian sector during solar minimum phases, *J. Geophys. Res. Space Physics*, *121*, doi:10.1002/2015JA022146.

Received 9 NOV 2015
Accepted 9 FEB 2016
Accepted article online 11 FEB 2016

©2016. American Geophysical Union. All Rights Reserved.

Disturbance zonal and vertical plasma drifts in the Peruvian sector during solar minimum phases

A. M. Santos[1], M. A. Abdu[1,2], J. R. Souza[1], J. H. A. Sobral[1], and I. S. Batista[1]

[1]National Institute For Space Research, São José dos Campos, Brazil, [2]Instituto Tecnológico de Aeronáutica, DCTA, São José dos Campos, Brazil

Abstract In the present work, we investigate the behavior of the equatorial *F* region zonal plasma drifts over the Peruvian region under magnetically disturbed conditions during two solar minimum epochs, one of them being the recent prolonged solar activity minimum. The study utilizes the vertical and zonal components of the plasma drifts measured by the Jicamarca (11.95°S; 76.87°W) incoherent scatter radar during two events that occurred on 10 April 1997 and 24 June 2008 and model calculation of the zonal drift in a realistic ionosphere simulated by the Sheffield University Plasmasphere-Ionosphere Model-INPE. Two main points are focused: (1) the connection between electric fields and plasma drifts under prompt penetration electric field during a disturbed periods and (2) anomalous behavior of daytime zonal drift in the absence of any magnetic storm. A perfect anticorrelation between vertical and zonal drifts was observed during the night and in the initial and growth phases of the magnetic storm. For the first time, based on a realistic low-latitude ionosphere, we will show, on a detailed quantitative basis, that this anticorrelation is driven mainly by a vertical Hall electric field induced by the primary zonal electric field in the presence of an enhanced nighttime *E* region ionization. It is shown that an increase in the field line-integrated Hall-to-Pedersen conductivity ratio $\left(\frac{\sum_H}{\sum_P}\right)$, which can arise from precipitation of energetic particles in the region of the South American Magnetic Anomaly, is capable of explaining the observed anticorrelation between the vertical and zonal plasma drifts. Evidence for the particle ionization is provided from the occurrence of anomalous sporadic *E* layers over the low-latitude station, Cachoeira Paulista (22.67°S; 44.9°W)—Brazil. It will also be shown that the zonal plasma drift reversal to eastward in the afternoon two hours earlier than its reference quiet time pattern is possibly caused by weakening of the zonal wind system during the prolonged solar minimum period.

1. Introduction

Electric field generation by neutral wind dynamo and the resulting currents and plasma drifts are fundamental parameters that control the electrodynamics of the terrestrial ionosphere. The ionospheric plasma drifts, in particular the vertical drift due to $\mathbf{E} \times \mathbf{B}$ force, has been a widely studied topic by the scientific community, since it allows a better understanding of the spatial and temporal distribution of the ionospheric plasma. In the equatorial region the interaction of the neutral atmospheric winds with the ionosphere under the nearly horizontal configuration of the geomagnetic field lines results in a unique daily variation of the equatorial electric field [*Haerendel et al.*, 1992].

The equatorial zonal and vertical drifts are driven, respectively, by the vertical and zonal electric fields along a magnetic flux tube. The quiet time vertical and zonal components of the dynamo electric fields cause the ionospheric plasma to drift westward and upward, respectively, during the daytime and eastward and downward at nighttime. During magnetic disturbances these drifts can be drastically modified by disturbance zonal electric fields of magnetospheric origin [e.g., *Kelley et al.*, 1979; *Kikuchi et al.*, 2008; *Abdu et al.*, 2009] and of disturbance ionospheric dynamos [e.g., *Blanc and Richmond*, 1890; *Abdu*, 1997; *Abdu et al.*, 2006; *Sobral et al.*, 1997; *Sastri*, 1988; *Scherliess and Fejer*, 1997; *Richmond and Lu*, 2000]. Many studies have investigated the influence of these disturbance electric fields on the vertical drift and related phenomena of the equatorial ionosphere, including the equatorial ionization anomaly (EIA), plasma structuring leading to bubble irregularities, equatorial electrojet current system, etc. [e.g., *Mannucci et al.*, 2005; *Abdu et al.*, 1995, 2003, 2007, 2009; *Batista et al.*, 1991, 2006; *Kikuchi et al.*, 2008; *Santos et al.*, 2012; *Sastri et al.*, 1993; *Sobral et al.*, 1997, 2001; *Tsurutani et al.*, 2008]. The effect of storm time penetration zonal electric field to produce large vertical

plasma drift, or superfountain, and dayside total electron content enhancement with resulting EIA intensification was reported by *Mannucci et al.* [2005] and *Tsurutani et al.* [2008]. Recent studies have revealed that the storm time disturbance zonal electric field that drives disturbance vertical drift can modify also the vertical electric field that drives zonal plasma drift with significant impacts on other equatorial phenomena such as the plasma flow dynamics, sporadic *E* layer (E_s) development, etc. [*Abdu et al.*, 2012, 2013, 2014]. *Abdu et al.* [2013, 2014] showed that a downward Hall electric field induced by a westward prompt penetration electric field during the nighttime, in the presence of an increase in the *E* layer conductivity, can produce a vertical ion velocity convergence sufficient to influence the formation of the E_s layer. On the other hand, an eastward prompt penetration electric field that dominates in daytime and at evening is able to induce an upward Hall electric field that can cause disruption/or weakening of an E_s layer. The influence of this same penetration electric field on the zonal plasma drift was discussed in *Abdu et al.* [2012]. The authors showed that while a disturbance westward electric field can cause an eastward/downward perturbation zonal drift, a disturbance eastward electric field can produces an upward perturbation in vertical drift that is accompanied by a westward perturbation in zonal drift.

Abdu et al. [1998] proposed a mechanism to explain the fluctuations in disturbed zonal plasma drifts observed during night at the *F* layer bottom side by a Canadian Advanced Digital Ionosonde over the equatorial station, Fortaleza [3,43°S; 38,52°W], as being caused by perturbations induced by disturbances in primary penetration zonal electric field. The zonal perturbation drift was driven by a vertical Hall electric field (induced by the primary prompt penetration zonal electric fields—PPEF) in the *E* region that was field line mapped to the *F* region through the equipotential magnetic field lines. For this mechanism to operate significant variations in the ratio of the Hall to Pedersen field line-integrated conductivities are necessary. For example, an increase in this ratio can arise from either a decrease in *F* region-integrated electron density (Pedersen conductivity) and/or an increase in *E* layer-integrated electron density (Hall conductivity), the latter arising, for example, from an extraionization produced by enhanced energetic particle precipitation that can occur in the South American Magnetic Anomaly region (SAMA) where the observation was made. In another work, *Abdu et al.* [2003] further confirmed the important role that this induced vertical Hall electric field plays (during nighttime) in the dynamics of the equatorial plasma bubbles over Brazilian sector and also in the formation and disruption of sporadic *E* layers in South American and Asian longitudes [*Abdu et al.*, 2014].

Several investigations on the zonal and vertical plasma drifts over Jicamarca, Peru, have revealed the different aspects of the dynamics of these drifts during quiet and disturbed periods [see, e.g., *Woodman*, 1972; *Fejer et al.*, 1981, 1985, 1991, 2005]. From the analysis of incoherent scatter radar measurements over Jicamarca, *Fejer and Emmert* [2003] observed an interesting case of daytime westward zonal plasma drift perturbation associated with an increase in its vertical drift that was caused by an eastward penetration electric field. Generation of Hall electric field by the PPEF under daytime conditions can occur easily due to the existing large daytime *E* layer Hall conductivity. Thus, this case represented a daytime manifestation of the Hall conduction effect in the *F* region, similar to the nighttime cases earlier reported by *Abdu et al.* [1998, 2003]. In the present work, we will analyze two cases of nighttime zonal and vertical drift perturbations during two magnetic storm events that occurred at the solar minimum activity years of 1997 and 2008, the latter representing a period of prolonged solar minimum activity. The zonal drift perturbations were modeled using the horizontal wind model (HWM93) and the zonal electric field measured by the Jicamarca radar coupled with field line-integrated parameters representative of a realistic low-latitude ionosphere as modeled by the Sheffield University Plasmasphere-Ionosphere Model (SUPIM) [*Bailey et al.*, 1993; *Bailey and Balan*, 1996; Bailey et al., 1997], which was modified at Instituto Nacional de Pesquisas Espaciais (INPE) to extend its lower height limit to 90 km (from the original limit of 120 km). We denote this as SUPIM-INPE. A comparison of the calculated results with the observations shows that a complete representation of the zonal drift perturbations is possible only when adequately enhanced Hall conductivity values (originating from *E* regions) were used in the calculations. Further, the study highlights the implication of the peculiar daytime zonal drift pattern on the zonal wind model used in this analysis. The impact of disturbance electric field on sporadic *E* layer development is also discussed. It is worth mentioning that detailed calculations like the present ones, regarding the behavior of disturbance vertical electric field/zonal drift have not been reported before.

2. Modeling the Zonal Plasma Drifts

The disturbance zonal drifts in the *F* region during two magnetic storm events as measured by incoherent scatter radar at Jicamarca (11.95°S; 76.87°W) were compared with the zonal drift calculated using a realistic

low-latitude ionosphere simulated by the SUPIM-INPE. The zonal velocities were calculated using the detailed formulations for ionospheric vertical electric field proposed by *Haerendel et al.* [1992]. We used a simplified expression for the same, as suggested by *Eccles* [1998] which is given by

$$E_L = \frac{\sum_H}{\sum_P}\left(BV_L - BU_L^H\right) - BU_y^P + \frac{L^{150}}{L}\frac{J_L^{150}}{\sum_P}, \quad (1)$$

where B is the total magnetic field intensity at the field line apex, $\sum_H$ and $\sum_P$ are the field line-integrated Hall and Pedersen conductivities, respectively. U_y^P is the field line-integrated and Pedersen conductivity weighted zonal wind velocity, U_L^H is the Hall conductivity weighted and field line-integrated meridional neutral wind velocity perpendicular to magnetic field B, V_L is the vertical plasma velocity in the equatorial plane, and J_L^{150} is the vertical current at $Z_{\mathrm{eq}} = 150$ km, where Z_{eq} is equatorial altitude. The coordinates used in this model electric field are L (the field line apex altitude in terms of Earth's radius (R_E), as given by $L = (R_E + Z_{eq})/R_E$) and y, which denotes the east-west component. L^{150} represents the parameter L for the apex equal to 150 km. Equation (1) was used without the third term, and the zonal plasma drift was calculated using the expression $V_y = E_L/B$.

2.1. Model Calculations

In order to calculate the zonal plasma drift, the field line-integrated parameters required to evaluate the electric field (E_L) were first calculated using SUPIM-INPE model results. The main input parameters for running this model are solar ionizing radiation flux, neutral atmospheric densities and temperatures, neutral winds, and the vertical plasma drifts. The EUV fluxes used in this study were obtained from SOLAR2000 model [*Tobiska et al.*, 2000]. The neutral gas concentration and temperature were represented by the NRLMSISE-00 atmosphere model. This empirical model is based on data collected from satellites, radars, and rockets (obtained mainly for the altitude below to 500 km) and can be used to describe on a global scale, for example, to make global predictions of temporal, daily, the diurnal, seasonal, latitudinal, and longitudinal variations of the neutral gases. The input parameters necessary to run the NRLMSISE-00 are year, day, time, geodetic altitude, latitude and longitude, the local apparent solar time, the 81 day average of $F_{10.7}$ solar flux, the daily $F_{10.7}$ solar flux for previous day and the daily magnetic index Ap [Picone et al., 2002]. The neutral wind velocity was obtained from horizontal wind model HWM93 [*Hedin et al.*, 1996]. The HWM93 is an empirical model based on observations collected from satellites and radars and provides the zonal and meridional components of the neutral wind as a function of local time, altitude, solar activity, latitude, and longitude. The vertical $\vec{E} \times \vec{B}$ plasma drift, another input parameter used in SUPIM-INPE, was that measured by the Jicamarca incoherent scatter. The *Scherliess and Fejer* [1999] empirical drift model (SF model) has also been used to complement the missing or inaccurate vertical drift data. For the magnetic storm of June 2008, the time interval for which the drift was complemented with SF model was between 2030 LT and 24 LT. For the April 1997 storm, this interval was from 1930 LT until 24 LT. The intensity of the Hall electric field that plays its role in the dynamics of the zonal drift was strongly dependent on the extraionization produced in the night E regions [*Abdu et al.*, 1998, 2003]. A source of extraionization in the form of energetic particle precipitation was introduced into the SUPIM input as explained below.

2.1.1. Inclusion of Extraionization Source by Energetic Particle Precipitation in the SUPIM-INPE Model

As the events studied here were observed in a region that is strongly affected by the SAMA, principally during magnetic storms, an additional ionization production by energetic electron precipitation was added to the otherwise dominant nighttime ionization production by the scattered EUV radiation as input to SUPIM-INPE model. The aim is to verify if this extraionization and therefore an increase in E region conductivity could explain the observed fluctuations in zonal plasma drift.

To evaluate the ion production by energetic electron precipitation it is necessary to know the energy spectrum of the precipitating particles. The vertical ionization profile due to monoenergetic precipitating electrons is given by [Rees, 1989]:

$$Q(z) = FE_p\Lambda\left(\frac{s}{R}\right)\frac{\rho(z)}{\Delta\varepsilon_{\mathrm{ion}}R\left(E_p\right)}, \quad (2)$$

where $Q(z)$ is the ionization rate per unit volume; F is the electron flux ($\mathrm{cm}^{-2}\,\mathrm{s}^{-1}$); E_p is the energy of monoenergetic electrons (eV); Λ is the energy dissipation function; s and R are the atmospheric depths in kilograms

per square meter (kg/m^2) at the altitude of interest and the effective range of the incident electrons also in kg/m^2, respectively; $\rho(z)$ is the mass density at altitude z; $\Delta\varepsilon_{ion}$ is the mean energy loss per ionization given by 0.035 keV [*Rees*, 1963]; and $R(E_p)$ is the maximum penetration depth. To calculate the ionization rate using equation (2), first, it was necessary to define an energy dissipation function for a beam of incident electrons, which was assumed to have an isotropic angular distribution with pitch angles varying between 0 to 80°. Other kinds of pitch angle distributions can be used, and as stated by *Rees* [1963] they have some effect in the ionization profiles but the energy dependence is found to be more important. According to *McDiarmid et al.* [1961], an isotropic angular distribution is the most commonly used one. The ion production rate due to energetic particle precipitation was calculated for a precipitating electron flux with the energy range similar to those used by *Abdu et al.* [2013], which was defined between 2 and 32 keV. The electron energy spectral shape was adapted from *Mann et al.* [1963]. The ionization due to precipitating particles was included in the SUPIM-INPE in the altitude range between 80 and 120 km by adding the additional ion production rate $Q(z)$ to the ionization produced by the scattered solar UV radiation already available in the model. Above the altitude of 120 km, a linear interpolation was used in order to make the ionization to decrease to the values unaffected by the precipitation. The electron density profile thus modified due to energetic particle precipitation was then used in the calculation of the field line-integrated Hall and Pedersen conductivity that are required to calculate the vertical electric field E_L using equation (1), as explained earlier.

3. Presentation of Results and Discussion

Two magnetic storms were selected during which the variations in zonal and vertical plasma drifts observed in the development phases of the storms were analyzed. The condition of the storms being in the development phase was very important because in this way any variation in drifts arising from disturbance winds could be largely excluded. The selected storm events occurred on 24 June 2008 and 10 April 1997 that corresponded to two solar minimum epochs, and the results of analysis will be presented in the following section.

3.1. The Magnetic Storm of 24 June 2008

Figure 1 shows the variations of the different interplanetary and magnetic indices during some days before and after June 24. It is possible to note a small auroral activity (*AE*) on 21 June (Figure 1, fourth panel), in which the *AE* index reached a maximum value of ~400 nT at ~10 UT. Regarding the interplanetary electric and magnetic fields E_y and B_z, only small fluctuations can be seen at the time of the *AE* fluctuations. Major activity started at the end of the day 24 June, when *AE*, B_z, and *SYM-H*/*Dst* indices reached values of ~800 nT, ~−6 nT and ~ −30 nT, respectively. Although this magnetic storm can be classified as "weak" [*Gonzalez et al.*, 1994], the vertical and zonal plasma drifts were found to be drastically modified in this day.

The vertical (V_z) and zonal (V_y) plasma drifts are presented in Figures 2d and 2e. The quiet time patterns of these drifts as per the models by *Scherliess and Fejer* [1999] (for V_z) and *Fejer et al.* [2005] (for V_y) are represented by the gray lines. The shaded area indicates the time interval during the storm development when an anticorrelation between V_z and V_y may be noted. The red arrows indicate the times of V_y eastward reversal according to experimental data and the drift model by *Fejer et al.* [2005]. The sunset time is indicated by the dotted vertical line. The *SYM-H*, B_z, and *AE* indices are also shown in this figure. We may note that B_z reverses weakly to south at 08 LT (13 UT) while the auroral index indicated mild activity that intensified slowly reaching a peak near 1630 UT. As to the drifts, we can see that during the day, V_z (Figure 2d) appeared very similar to a quiet day, except for some minor disturbances, while V_y also presented a nearly quiet time behavior, but until to 13 LT (18 UT). After this, a great discrepancy can be noticed between the observed zonal drift and model zonal drift from *Fejer et al.* [2005]. Especially, the afternoon reversal of the drift to east occurred 2 h earlier than such reversal in the quiet day model drift, as indicated by the red arrows. These results show a strong evidence that the zonal drift model from *Fejer et al.* [2005], which is an average drift, is not representative of what is expected from the zonal wind (one of the drivers of the zonal plasma drift during the day) for the present observational epoch. Also, it is interesting to note that this variation in the zonal drift occurred in the absence of any significant magnetic storm. The possible causes for this difference will be discussed latter. Also, in Figure 2, we may note that the B_z remained southward from 08 LT (13 UT) until 1330 LT (1830 UT) and then reversed to north followed by fluctuations that hardly produced any effect in the plasma drifts over Jicamarca. Notable effects over Jicamarca set in with a definitive and rapid B_z inversion to southward at 1730 LT (2230 UT) that was soon followed by an increase in auroral activity. We may note that V_z presented small

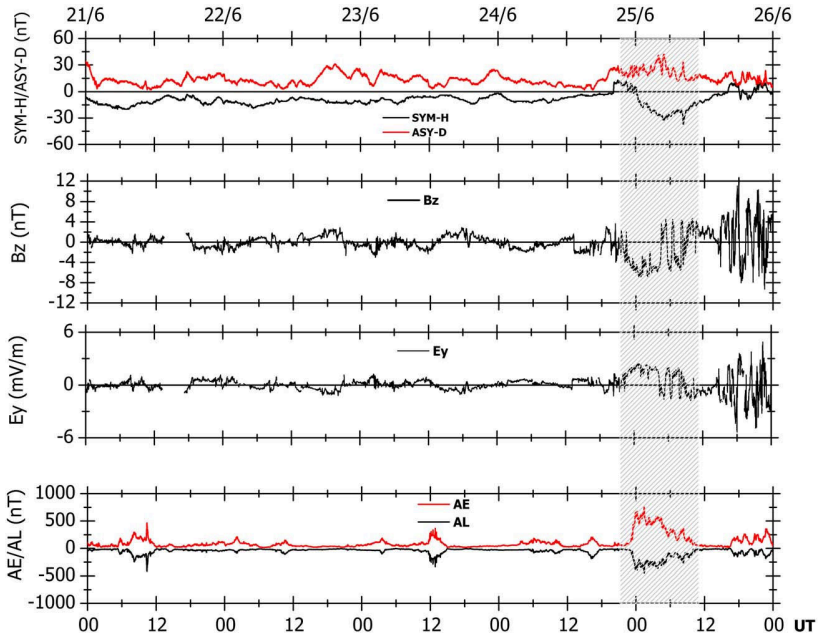

Figure 1. Variation of magnetic indices during the period of 21 to 25 June 2008. The indices are the (first panel) *SYM-H/ASY-D*, the (second panel) IMF-B_z from ACE satellite, (third panel) the electric field E_y and the (fourth panel) *AE/AL* indices. The shaded area indicates the interval in which remarkable fluctuations were observed in the vertical ad zonal drifts.

amplitude fluctuations during this period until it suddenly increased at 1830 LT (2330 UT) to reach an amplitude of ~30 m/s at 19 LT (00 UT). This increase in the vertical drift was caused by a prompt penetration (undershielding) eastward electric field associated with the *AE* development under B_z south conditions. In the following instants, the *AE* partial recovery (during 00–0040 UT) is coincident with a decrease in V_z that can be associated to an overshielding condition. The vertical drift for quiet days (gray line, Figure 2d) shows the complete absence of an evening prereversal enhancement (PRE), a behavior that is characteristic of this time of the year (June solstice) over Jicamarca.

The *SYM-H/Dst* index reveals that the effects of this magnetic storm in the equatorial ionosphere over Jicamarca began well before the onset of the storm main phase. It is possible to observe that the zonal drift V_y (Figure 2e) reversed to east at ~ 15 LT (~20 UT) and between 17 LT (22 UT) and 1750 LT (2250 UT) shows a clear tendency of stabilization at around 50 m/s. This tendency is interrupted after 1750 LT (2250 UT), when a decrease in the eastward V_y can be noted (as indicated by the dotted line near sunset). This decrease can be associated to a perturbation in the primary zonal electric field as evidenced by the increase in V_z at the same time. It is possible that this perturbation induced a vertical Hall electric field in *E* region, which when mapped to *F* region, produced a disturbance in the zonal plasma drift over this region. Starting at 19 LT (00 UT), the rapid decrease in V_z that was associated with the partial recovery in the *AE* index (as pointed out above) was accompanied by a strong increase in zonal drift to east, which reached a peak of 60 m/s near 20 LT (01 UT).

The variations in the zonal and vertical plasma drifts presented here highlight two main points to be investigated. First, it is necessary to explain the afternoon eastward reversal of the zonal plasma drift 2 h before its expected/modeled reversal time, considering that this important variation occurred without any magnetic disturbance. Since it is a quiet time feature related possibly to the extreme and long duration solar minimum conditions of the recent solar cycle, this is being addressed in a separate paper. The other important point that must be examined is the physical mechanism responsible for the anticorrelated variations between zonal and vertical plasma drifts during the development/growth phase of a magnetic storm. In order to address this point, the SUPIM-INPE was used to model the equatorial ionosphere over Jicamarca, which will be discussed in the next section.

3.1.1. Ionospheric Model Validation

A realistic electronic density latitude height distribution is required to calculate the field line-integrated parameters needed to obtain the vertical electric field (that is, the zonal drift) (as per equation (1)). The critical

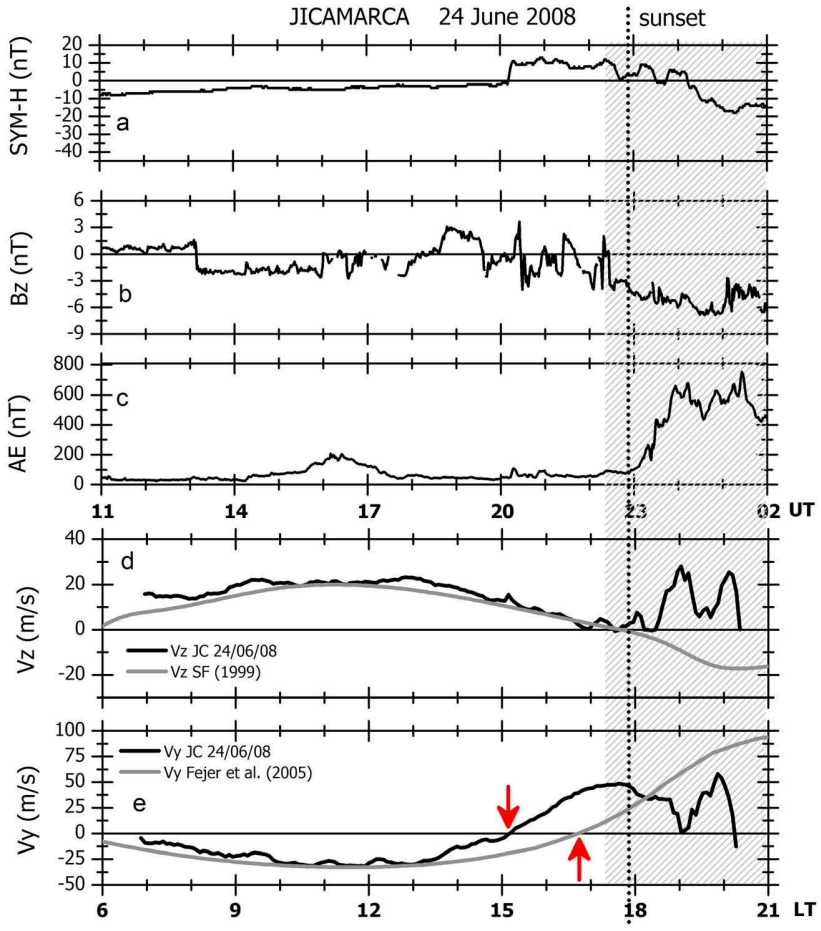

Figure 2. The (a) *SYM-H*, (b) B_z, and (c) *AE* variations during 24 June 2008. The (d) vertical (V_z) and (e) zonal (V_y) plasma drifts measured by the ISR from Jicamarca are presented (black curves).

frequency of the *F* layer (f_oF_2) which represents the electron density at the *F* layer peak height (h_mF_2) can be considered as indicative of the electron density distribution along a flux tube whose apex height coincides with the h_mF_2 over the dip equator. Thus, the verification that the f_oF_2 values over Jicamarca obtained from the model is in agreement with the experimental data is very important to lay confidence in the field line-integrated parameters obtained by SUPIM-INPE model. Figure 3 shows a comparison between the modeled and observed f_oF_2 values. The experimental data are indicated by the black line, in which the solid/dotted segments represent the values of f_oF_2 measured in the absence/presence of spread *F*. (The f_oF_2 measurement in the presence of spread *F* is not always reliable). In view of an expected impact of the deep solar minimum of 2008 on the solar irradiance control of the ionospheric electron density, some adjustments in the solar irradiance model, SOLAR2000, was necessary in order to obtain a more satisfactory result on the f_oF_2. The details of these adjustments will be discussed in a separated paper. The final model results are shown by a red curve. It is possible to observe an excellent agreement between the modeled and observed f_oF_2 values, except during 01–06 UT when spread *F* was present in the ionograms. We know that during this interval, the spread *F* trace must have caused error in the reading of f_oF_2 in ionograms (usually leading to its overestimation). A possible influence of a disturbance electric fields, considering the fluctuations of the B_z (dominantly to south) during this time (see Figure 1), which is to cause most likely a decrease in f_oF_2, has been masked by the interference from spread *F* trace. Since this study focuses on the time interval in which the fluctuations in the drift was observed (between ~18 UT and ~01 UT), we believe that the discrepancy between modeled and observed data in some intervals after this time does not affect our results.

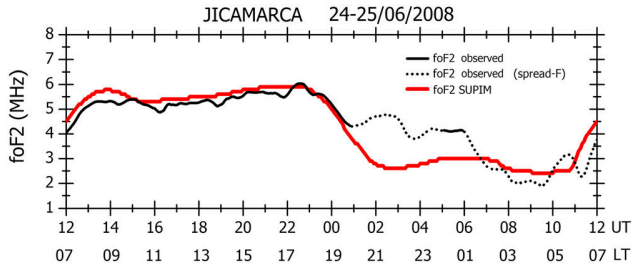

Figure 3. Comparison of critical frequency of the *F* layer (f_oF_2) registered by the Digissonde at Jicamarca and the f_oF_2 modeled by SUPIM-INPE model. The black dotted line indicates the f_oF_2 parameter processed in the presence of spread *F* traces.

3.1.2. Comparative Analysis Between the Zonal Drift Observed and That Calculated Using the SUPIM-INPE Model

The zonal plasma drift velocities calculated considering the field line-integrated parameters for an apex height of 400 km is shown in Figure 4. For this case the parameter J_L (in equation (1)) was not included in the calculation of zonal drift. In agreement with *Haerendel et al.* [1992] the vertical current is only important at sunset time and below the *F* layer peak. *Eccles* [1998] ignored this term in his development a simple low-latitude electric field model.

Figure 4 shows from the top to the bottom the ratio $\frac{\sum_H}{\sum_P}$ (a), the vertical (b), and zonal plasma drifts (c and d) and the calculated zonal plasma drift (c and d) for three different conditions. The dashed blue line indicates the zonal drift considering only the wind term U_y^P. The velocity in this case is given by [*Eccles*, 1998]:

$$V_y = U_y^P = \frac{\sum_P^E U_y^{PE} + \sum_P^F U_y^{PF}}{\sum_P^E + \sum_P^F}, \tag{3}$$

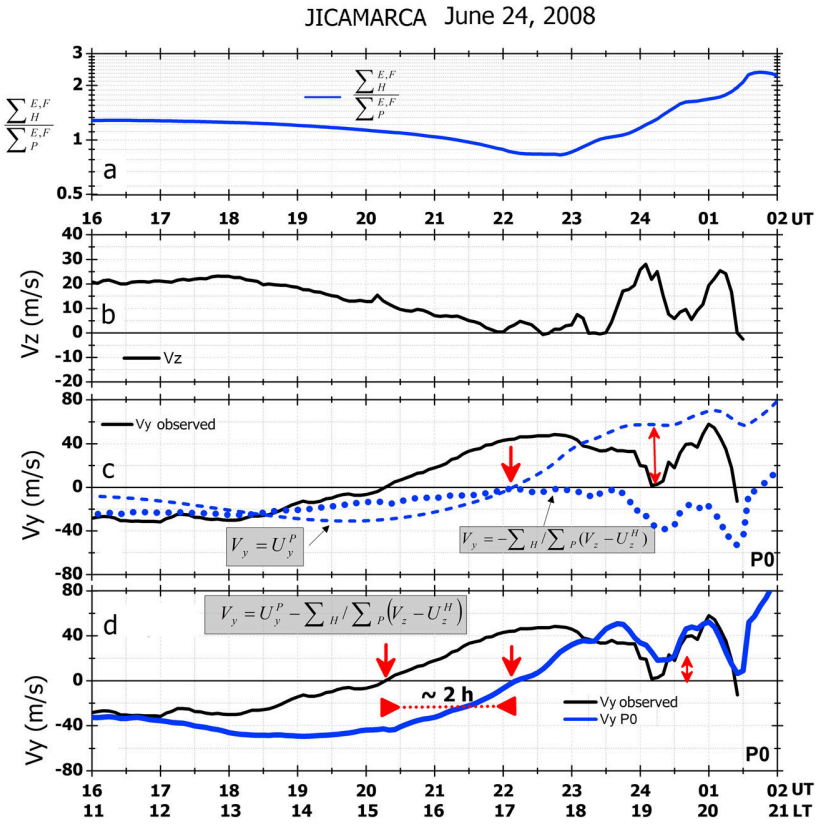

Figure 4. (a) Hall-to-Pedersen conductivity ratio $\frac{\sum_H}{\sum_P}$, (b) the vertical drift V_z, and (c and d) the zonal drifts (V_y) during 24 June. The calculated zonal drifts for different conditions are also presented as solid, dotted, and dashed blue line in Figures 4c and 4d. The red arrows indicate some important points that are discussed in the text.

where U_y^{PE} and U_y^{PF} corresponds to zonal wind from the *E* and *F* regions, respectively, weighted by Pedersen conductivity along the corresponding field line segments. The blue dotted curve represents the component of the zonal drift arising from the parameter $-\frac{\sum_H}{\sum_P}(V_Z - U_Z^H)$. In Figure 4d, we show the sum of the zonal drift arising from both the zonal wind and the Hall conduction terms together, i.e., $U_y^P - \frac{\sum_H}{\sum_P}(V_Z - U_Z^H)$. Three different features can be noticed when a comparison is made between the calculated zonal drifts (blue curves) and experimental data (black line) in Figures 4c and 4d. First, we note in Figure 4c that between ~1830 UT and 2330 UT, the discrepancies between the drifts seem to be caused mainly by the zonal wind, since the contribution of the term $-\frac{\sum_H}{\sum_P}(V_Z - U_Z^H)$, which includes dominantly the values of V_z, is small for most of the duration. At ~ 2210 UT, for example, this term attained a value of ~ −1.2 m/s only. The second feature is that the oscillations in V_y observed between 2330 UT and 0130 UT can be simulated only if the parameter that involves V_z is considered. When we compare the dashed line in Figure 4c with observed drift (solid black line) at 0010 UT, we note a difference of ~60 m/s (as indicated by the vertical red arrow), but when this comparison is made between the drifts in Figure 4d, this difference gets reduced to ~20 m/s. The last feature to be noticed is related to the time at which the afternoon zonal drift reverses to east. As observed in Figure 2, the model result in Figure 4 presents a discrepancy of ~ 2 h with respect to the times at which the zonal drifts reverse to east; that is, the observed zonal drift reverses to east 2 h earlier than the calculated drift. In other words, the model zonal wind (HWM93) used in the drift calculation is not representative of the wind that drives the observed zonal drift during a long interval of the day. Furthermore, the difference of ~20 m/s between the drifts detected at 0010 UT (Figure 4d, indicated by red arrows) shows that there may have been an additional factor influencing the zonal drift fluctuations. As indicated by the first two terms in equation (1), the different factors that could affect the vertical electric field/zonal drift are the modification in the integrated conductivities, in the zonal electric field/vertical drift, and in the zonal winds.

3.1.3. Zonal Drift Variation Considering Modified Zonal Wind and an Extraionization Due To Energetic Particle Precipitation

In order to clarify the disparity identified between the observed and calculated zonal drifts, two factors were investigated: the zonal wind and the energetic particle precipitation. We believe that a suitably modified zonal wind should explain the earlier reversal of the drift to east. Additionally, an increase in the Hall conductivity due to enhanced ionization by particle precipitation could contribute significantly for the zonal drift minimum observed at 0010 UT to be better represented by the model.

The zonal drift according to equation (3) that is plotted in Figure 4 (dashed line in c) is the representative of conditions in the absence of any significant magnetic activity. The equation (3) suggests that the differences in these drift variations with respect to the observed zonal drift can possibly be caused by the assumed zonal wind as well as by the integrated Pedersen conductivity; obviously, this is valid for the period before the beginning of the storm. Since the *F* region electron density modeled by the SUPIM-INPE shows good agreement with observational data (see Figure 3), we expect the spatial and temporal distribution of the conductivities to be very close to being correct, and therefore, we believe that the differences found in the drifts should be caused mainly by the zonal wind model (HWM93) used in the calculation. This point is further supported by the well-known fact that the thermospheric winds present great variability and affect directly the ionosphere in all latitudes. Furthermore, as mentioned by *Biondi et al.* [1999] the main factors that control the thermospheric circulation are the EUV flux, the location of subsolar point, the Earth rotation, and also the dissipation of gravity waves and ion drag. As the analysis presented here refers to a period of extreme solar minimum activity and as the radiation in EUV was 15% less in 2008 in relation to the previous solar minimum [*Liu et al.*, 2012] it seems reasonable to consider that the zonal wind had a great influence in the earlier inversion of zonal drift to east. In addition, as the lower is the $F_{10.7}$ index, the lower will be the atmospheric pressure gradient with the subsolar point in the ionosphere domain; and therefore, the lower will be the zonal wind velocity generated by the solar thermal tide. Under this situation, the eastward corotational force may help the eastward wind velocity reversal to occur earlier. Thus, it is clear that the model wind HWM93 does not adequately represent this year of very low solar activity. Therefore, some adjustments were implemented in the zonal wind so that the calculated zonal drift could be as close as possible to the observed zonal drift. It is important to mention that adjustments were carried out between 16 UT and 2330 UT, during which the magnetic activity was absent. After this time, we note that the variation pattern of the calculated drift (Figure 4d) is consistent with that of the observed drift but with a different magnitude. Basic adjustments

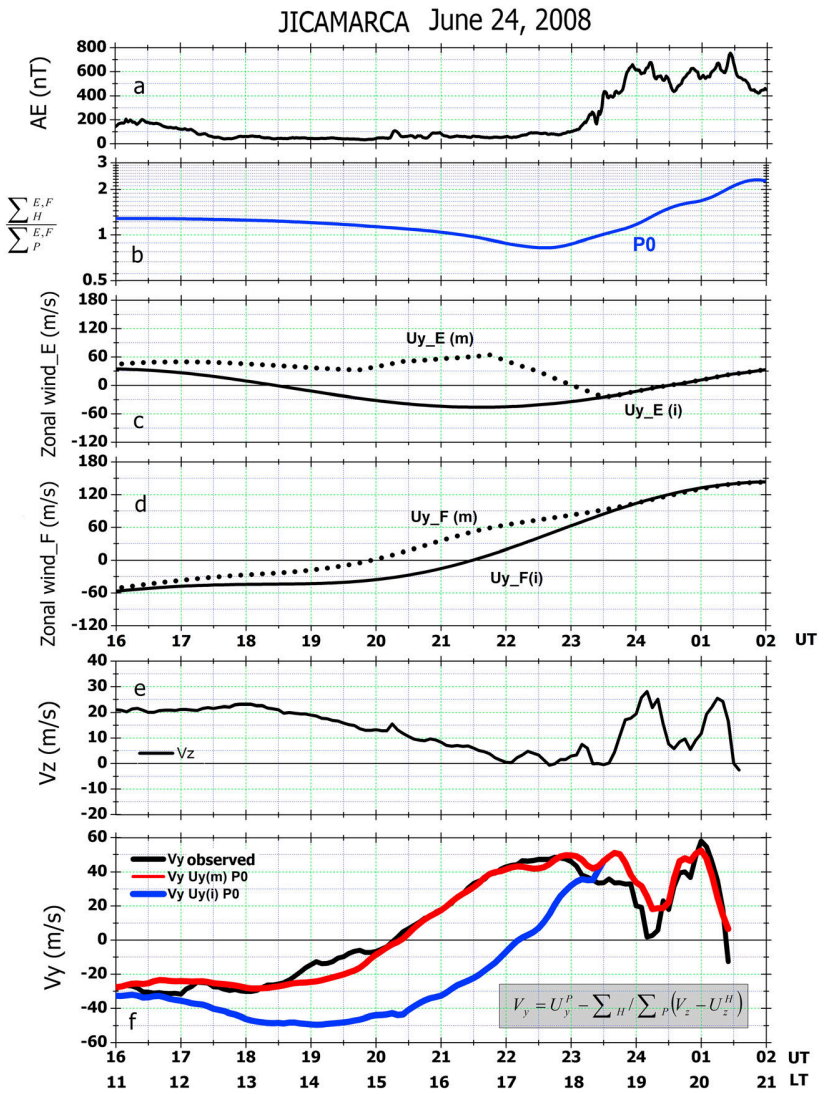

Figure 5. The (a) auroral activity, the (b) ratio $\frac{\sum_H^{E,F}}{\sum_P^{E,F}}$, the initial $U_y(i)$ and modified $U_y(m)$ zonal wind of the regions (c) *E* and (d) *F*, the (e) vertical drift V_z, and the (f) experimental and calculated zonal drifts. The red/blue curve in panel f indicates the calculated zonal drift considering/not considering the correction in zonal wind.

were effected in the winds by adding to the HWM93 a time varying wind that resulted in the calculated drift to reverse eastward at the same time, 2020 UT, as the reversal time in the observed drift. The result of this modification in zonal drift is presented in Figure 5, which shows from the top to the bottom the auroral activity (*AE*), the Hall to Pedersen conductivity ratio, the initial $U_y(i)$ and the modified zonal wind $U_y(m)$ of the *E* and *F* regions, the vertical drift V_z, and finally, the calculated (red and blue curves) and observed (black curve) zonal drift V_y. In Figures 5c and 5d we can verify that after 23 UT, the behavior of $U_y(m)$ is very similar to $U_y(i)$. In Figure 5f, the red/blue curve represents the calculated zonal drift with/without modifications in zonal wind. As a result of the modification in the zonal wind we have obtained an excellent agreement between the red and black curves, mainly during the time interval in which the zonal drift reverses to east. Also, it is interesting to note that in the case in which the drift was calculated considering the initial wind (blue curve), the reversal of the drift to east occurred ~40 min after the reversal of the *F* region zonal wind (Figure 5d, solid curve), while the delay between the reversal time in the modified wind, $U_y(m)$, and that in the corresponding zonal drift is only ~15 min.

In addition to the modification introduced in the zonal wind system, other adjustments were necessary in order to find more satisfactory results. It may be noted in Figure 5f that the fluctuating zonal drift reached

a value of ~0 m/s at ~0010 UT, which was coincident with a peak in the auroral activity. So in this context, we cannot assume that the wind was responsible for this modification in zonal drift, since there would not be enough time for a disturbance wind to reach equatorial latitudes. Considering that the winds were unperturbed for a short period after 2300 UT (at which a magnetic storm began, as indicated by the *AE* index in Figure 5a), we believe that the observed modifications in the zonal drift must be caused by an increase in the ratio $\frac{\sum_H}{\sum_P}$, which could arise from ionization enhancement in the *E* region due to storm associated energetic particle precipitation. Ionosonde data from Cachoeira Paulista, Brazil, detected the occurrence of anomalous sporadic *E* layers in ionograms (to be discussed later), which may be considered as a strong indicator of energetic particle precipitation in this general region. In view of the fact that particle precipitation in the *E* region could enhance the conductivities and therefore the ratio, $\frac{\sum_H}{\sum_P}$, it was necessary to make some tests with SUPIM-INPE model to determine an energy spectra that could generate a zonal drift coherent with the experimental data.

Figure 6d shows the results for the resulting zonal drifts. The blue curve, identified as $V_y\ U_y(m)P_0$, represents the zonal drift obtained when the zonal wind only was modified. The red curve, identified as $V_y\ U_y(m)P_1$, represents the zonal drift obtained when, beside the modified zonal wind, an increase in the ratio $\frac{\sum_H}{\sum_P}$ due to enhanced particle precipitation was also included. Here the indices P_0 and P_1 indicate, respectively, the inclusion and noninclusion of the energetic particle precipitation in the calculation. Comparing the observational data (black curve) and the model results indicated by the red curve, we note an excellent agreement between the drifts during the entire period available. We may further verify that the excellent agreement between 00 UT and 0030 UT was only possible when the $\frac{\sum_H}{\sum_P}$ ratio during this period was increased from 1.25 to 1.5 (see red curve, P_1, of Figure 6b). This increase was generated by an electron flux that varied from 9.4×10^3 el cm^{-2} s^{-1} to 2.4×10^3 el cm^{-2} s^{-1} in the energy range from 2 to 32 keV.

It is interesting to note in Figure 6 that the decrease in zonal drift observed near 00 UT was exactly coincident with an increase in the vertical drift. We believe that this intensification in the vertical drift, which was caused by a prompt penetration electric field to the east, produced a vertical Hall electric field in the night *E* region under enhanced Hall conductivity (due to energetic particle precipitation). This upward vertical electric field, when mapped to the *F* region, was responsible for the decrease in the eastward zonal drift that occurred at this time.

The energy spectra used in the calculation that yielded the excellent agreement discussed above was based on measurements made by the Discovery 29 satellite in a passage over SAMA region. For the energy range used in our study (2–32 keV), it was necessary to make an extrapolation in the electron energy spectral shape from that reported by *Mann et al.* [1963] in order to include important levels for *E* region. Since we did not find measurements of electron flux for this specific event studied here, we made an indirect verification of the consistency of the energy spectra used in our calculation by comparing the electron flux used in our analysis with the electron flux used by *Del Pozo et al.* [1997] for the auroral region. The result of this comparison showed that the values used by us were lower by ~ 5 orders of magnitude. Therefore, we believe that the flux values used in this work may be reasonable and consistent with an electron flux expected in the SAMA region.

As mentioned previously, the calculation of the zonal drift was made numerically in the field line with an apex height of 400 km, which intercepts the low-latitude *E* layer at ~ ± 12°. In order to verify the effect of particle precipitation on the Hall and Pedersen conductivities, Figure 7 was constructed to show the profiles of these conductivities over these latitudes with and without precipitation. The solid line represents the conductivity height profiles without particle precipitation (P_0) while the line with circles represents the conductivities including the precipitation (P_1). We may note that in agreement with the precipitation spectra chosen, the inclusion of the precipitation was restricted to the *E* region and affected both Hall and Pedersen conductivities. Therefore, as the Hall conductivity is higher at lower layers of the ionosphere, the effects of the particle precipitation is to increase the integrated values more significantly for the Hall conductivity, thereby leading to enhanced ratio of the integrated Hall-to-Pedersen conductivities.

3.1.4. Evidences for Ionization Increase in the Night *E* Region in Ionograms

The ionograms recorded by Digisondes are important tools that allow verifying the presence of indicators of energetic particle precipitation in the ionosphere. As shown above, the inclusion of an extraionization by

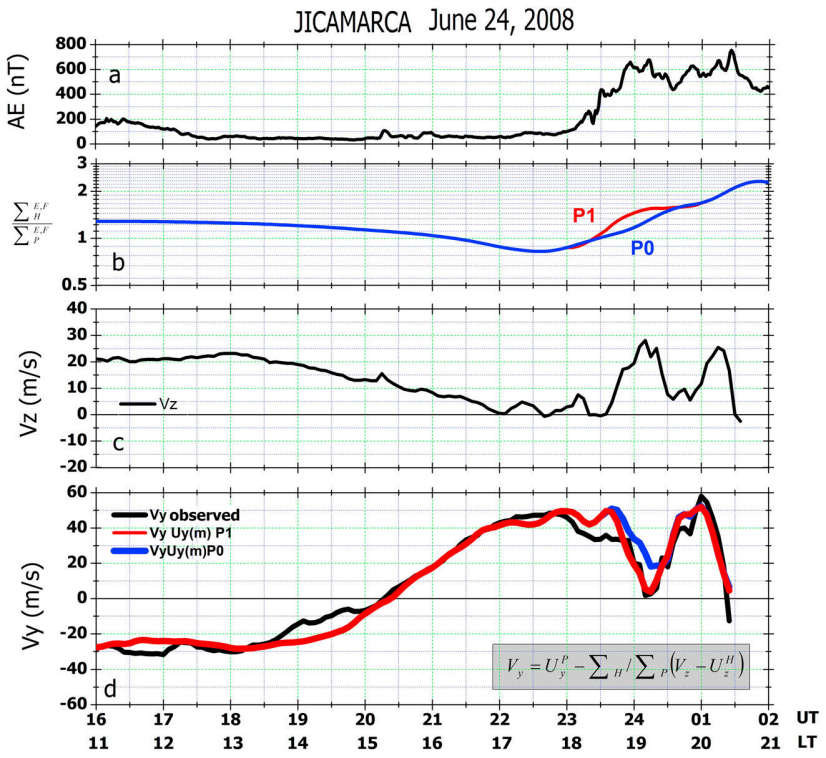

Figure 6. The (a) auroral activity, the (b) ratio $\frac{\sum_H}{\sum_P}$ including (red curve) or not including (blue curve) the particle precipitation, the (c) vertical drift V_z, and the (d) experimental and calculated zonal drift considering only the correction in zonal wind (blue curve) and considering the correction in zonal winds + precipitation particle (red curve).

particle precipitation was a key factor to explain some fluctuations in the zonal drift. It is important to mention that since all the parameters involved in the calculation of the zonal drift refer to field line-integrated ones, the ideal approach would be to check evidence for particle precipitation occurring in the low-latitude *E* region field line mapped to equatorial apex height over Jicamarca around 400 km. As there is no Digisonde installed in these regions (±12° latitude), we use data from Cachoeria Paulista as reference.

It is well known that ionization enhancement in the *E* region can be detected from the characteristics of sporadic *E* layers especially when they occur in the nighttime ionosphere over the region of the SAMA *Abdu et al.*, [2005]. *Batista and Abdu* [1977] and *Abdu et al.* [1981] investigated the E_s over Cachoeira Paulista during some events of magnetic storms and noted that the pattern of the E_s layer exhibited significant degree of range spreading in the echoes very similar to that of the *a*-type E_s layer known to occur over auroral latitude. The result over Cachoeira Paulista was interpreted as strong evidence for ionization enhancement in the *E* region caused by energetic particle precipitation in the SAMA region.

Figure 8 shows the ionograms over Cachoeira Paulista on 24 June. As indicated by the blue vertical arrow, the critical frequency of the *F* region (f_oF_2) at 2330 UT is very low (around ~3 MHz) and decreases afterward. It is possible to note that the E_s layer trace in ionograms exhibits a range spreading in the echoes indicating that its formation can be associated to the particle precipitation. In some ionograms, such as those at 2245 UT and 2330 UT, it is possible to note a tendency of group delay (in the form of minor curvature) at the lower frequency end of the *F* layer trace, similar to that observed also over Jicamarca (not shown here) which is indicative of presence of ionization in the region below the *F* layer.

At 00 UT (21 LT), the ionosphere was under strong influence of a penetration eastward electric field as indicated by the intensification in vertical drift between 2330 UT (2030 LT) and 0015 UT (2115 LT) in Figure 2. At this time, we note the almost complete disappearance of the *F* layer trace, which was caused by the "blanketing-type" E_s layer that developed during this period. The observed E_s layer transformation/intensification represent an

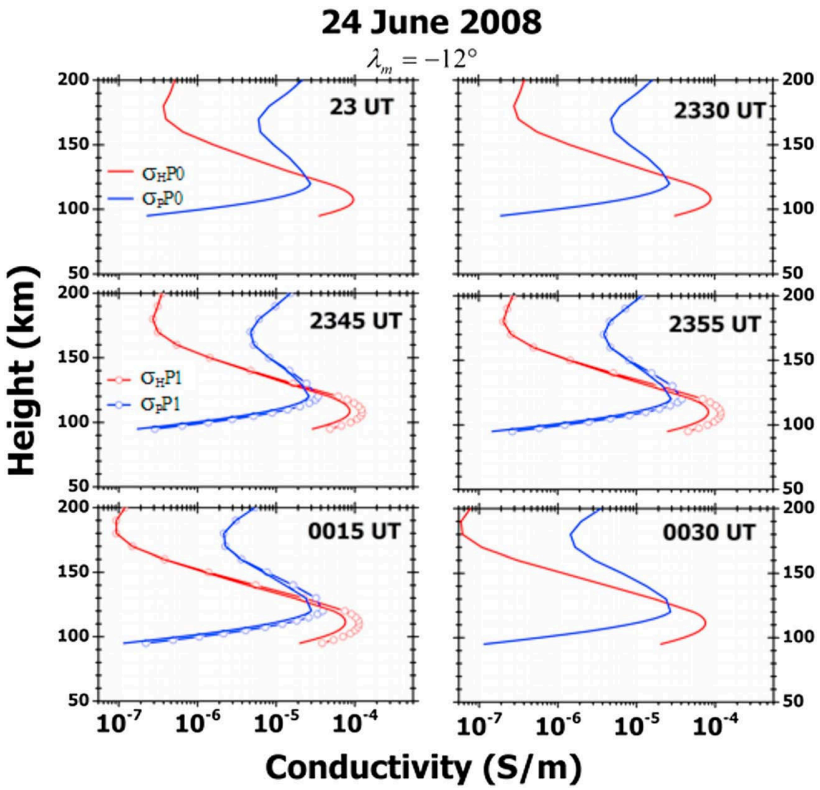

Figure 7. Profiles of Hall (red curves) and Pedersen (blue curves) conductivities including (P_1, circle curves) or not including (P_0, solid curves) the particle precipitation for a magnetic latitude of −12° during 24 June. The particle precipitation was only included between 2345 UT and 0015 UT.

enhancement in the *E* region electron density likely caused by the extraionization produced by the precipitation of energetic particle.

Starting at 00 UT, it is interesting to note the presence of two traces located at ~100 km and in ~130 km and also the beginning of the second hop for the E_s at 130 km. At 0030 UT, the lower trace was nearly disrupted while the E_s at ~130 km continued with its second hop trace until 0230 UT. The intensification of the E_s at 130 km at 0015 UT is coincident with the beginning of a decrease of the vertical drift caused by a superposed westward penetration electric field. Between 02 UT and 0230 UT, the ionograms show periods of intensification, decay, and also rupture of this sporadic layer. The rupture of the lower E_s with spread at 0030 UT was coincident with end of the descent in the vertical drift. Thus, while there is evidence, though qualitatively, for the role of energetic particle precipitation in the E_s layer formation, the variability in the intensity and structuring of these layers can be, and indeed appears to be, influenced also by the fluctuating penetration electric field. It is also important to note that the conditions of background winds [*Whitehead*, 1970; *Mathews*, 1998] as well the integrated conductivities in the field lines of their occurrence [*Abdu et al.*, 2014] could significantly influence the dynamics of these layers. These will be the focus of a separate investigation. The important point to be highlighted here is that an enhanced ionization (due to energetic particle precipitation) as evidenced by the anomalous E_s layer formations, constitute an important element toward reaching agreement, in a quantitative way, between the observed and modeled zonal plasma drift during magnetic disturbances.

3.2. The Magnetic Storm of 10 April 1997

During the magnetic storm of 10 April 1997, the *F* layer zonal plasma drift, as measured by the Jicamarca ISR, showed a complete reversal to westward, near sunset, under the strong influence of the magnetic disturbances that started around the same time, as can be seen in the results presented in Figure 9. As in the case presented previously, any role of disturbance winds can be neglected in this case as well. This figure shows, in

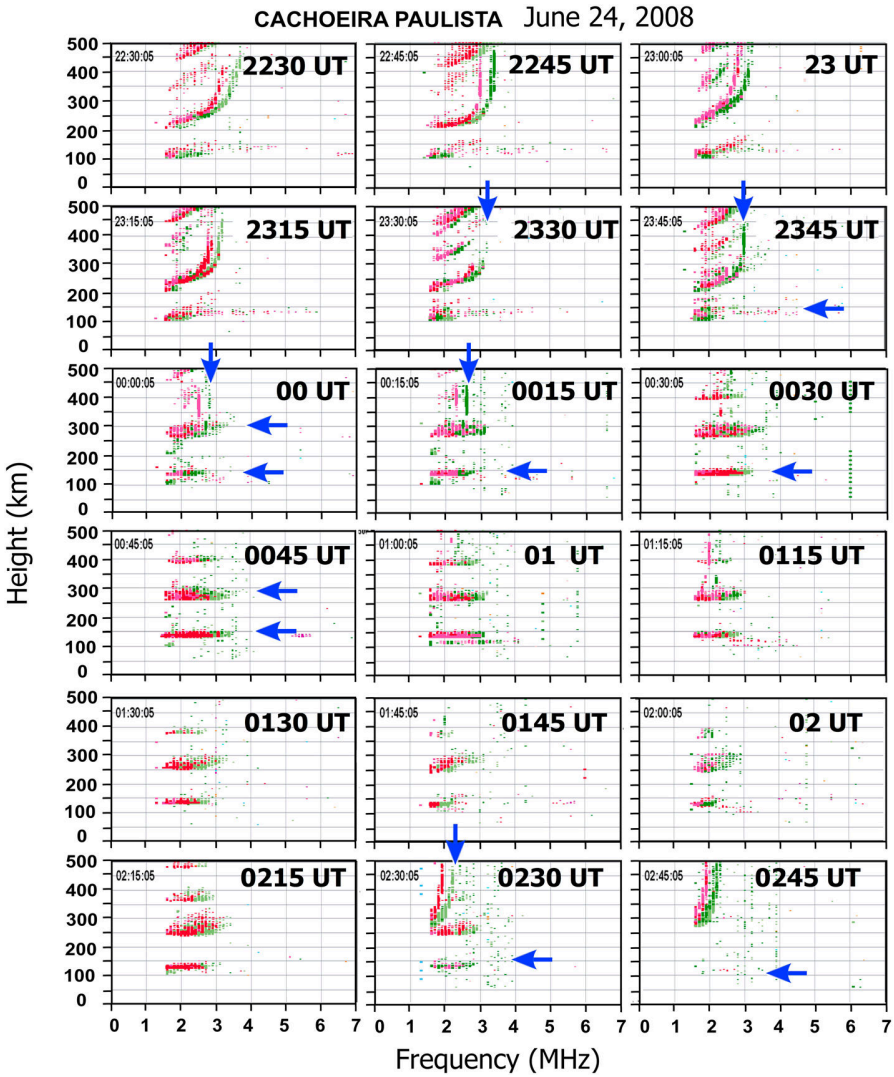

Figure 8. Ionogram sequence for Cachoeria Paulista on 24 June. The vertical blue arrows show the reductions in the f_oF_2 parameter, while the horizontal arrows show the presence of sporadic layers.

the top three panels (a, b, c) the magnetic indices, *SYM-H*, B_z, and *AE*, and in the bottom two panels (d, e) the vertical and zonal plasma drifts over Jicamarca. In Figure 9e, we note near 19 LT an anomalous reversal to west in the zonal drift when we expected an intense zonal drift to east (~100 m/s) as expected from its quiet day pattern (gray curve). At about the same time it is observed that the vertical drift around the PRE was significantly modified following a rapid intensification in the auroral activity under B_z south condition. The *AE* index reached a value of ~1200 nT at ~23 UT and soon after presented a partial recovery attaining a level of ~900 nT that continued for ~1 h and 10 min. During this time, the vertical drift showed large increase attaining 50 m/s, at 00 UT, which was superimposed on quiet time PRE (the average quiet time PRE amplitude is ~15 m/s as shown by the grey curve in Figure 9d). This was caused by an undershielding penetration electric field of eastward polarity associated with the *AE* activity under B_z south condition. We may note that at the same time (~1 h after the start of increase of V_z), the zonal drift reversed westward attaining a value of ~ −50 m/s at 0010 UT. A rapid and transient recovery in the B_z soon after 00 UT, appears to have produced an abrupt decrease (and reversal to downward) in V_z, which was accompanied by a rapid eastward recovery in zonal disturbance drift that continued for about one hour. Thus, this event is yet another example of an under-shielding electric field that modified the vertical plasma drift, at the same time inducing a vertical Hall electric field that drove the zonal plasma drift to westward. This event also occurred in a period of solar

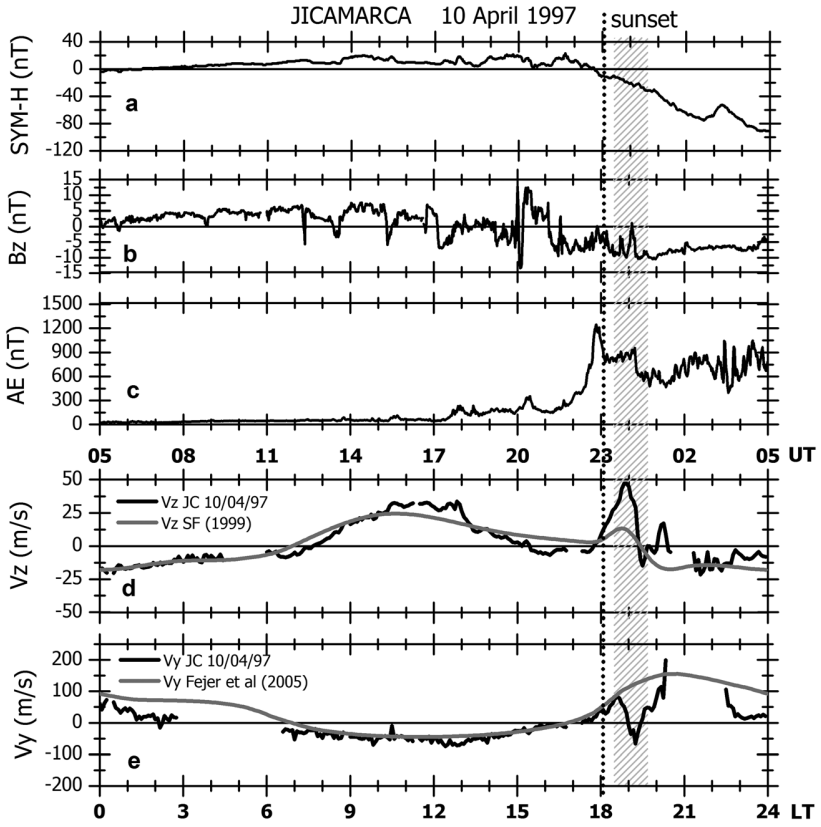

Figure 9. The (a) *SYM-H*, (b) B_z, and (c) *AE* time variations on 10 April 1997. The (c) vertical (V_z) and (d) zonal (V_y) plasma drifts measured by the ISR from Jicamarca are presented (black curves). The quiet day reference drift is plotted by gray curve and was obtained from models of *Scherliess and Fejer* [1999] (V_z) and *Fejer et al.* [2005] (V_y). The shaded area shows the anticorrelation between V_z and V_y associated with the beginning of a magnetic storm. The sunset time is indicated by the dotted vertical line.

minimum, but unlike in the event of June 2008, the zonal drift reversal to eastward in the afternoon occurred at the same time (black curve) as it did in the quiet day reference curve (gray curve—*Fejer et al.* [2005]). This is a clear indication that the HWM93 does appear to describe well the quiet time zonal wind during this solar minimum epoch, whereas, in contrast, it does not describe well the zonal wind under the prolonged extreme solar minimum conditions represented by the June 2008 epoch.

Figure 10 shows plots related to the modeling procedure adopted for this event together with some observational data. It presents in panels from top to bottom: the *AE* index (Figure 10a), the integrated Hall and Pedersen conductivity of the *E* and *F* regions (Figure 10b), the ratio $\frac{\sum_H}{\sum_P}$ (Figure 10c), the zonal winds from the *E* and *F* regions (Figures 10d and 10e), the vertical drift (Figure 10f) and the zonal plasma drifts (Figures 10g and 10h). We may note that the calculated zonal drift considering only the zonal wind, that is, the conductivity weighted field line-integrated zonal wind ($V_y = U_y^P$, Figure 10g) shows reasonably good agreement with observed data during the day, thereby suggesting that the winds used in the calculations are appropriate, not warranting any unique/specific adjustments. However, at the time of the anticorrelation between V_y and V_z near ~19 LT, (in Figures 10f and 10g) we may notice only a small contribution from this term. On the other hand, when V_y was calculated by including the terms in the winds as well as the conductivity ratio, (Figure 10h), a better coherence between the calculated and the observed drifts was obtained for all the interval studied, especially during the evening hours around the PRE. As to the values of $\frac{\sum_H}{\sum_P}$, we may note that between 12 UT and 2330 UT this ratio has a value of ~1, however, from 2330 UT a significant increase in this ratio can be identified (Figure 10c). Such increase is caused by the faster Pedersen

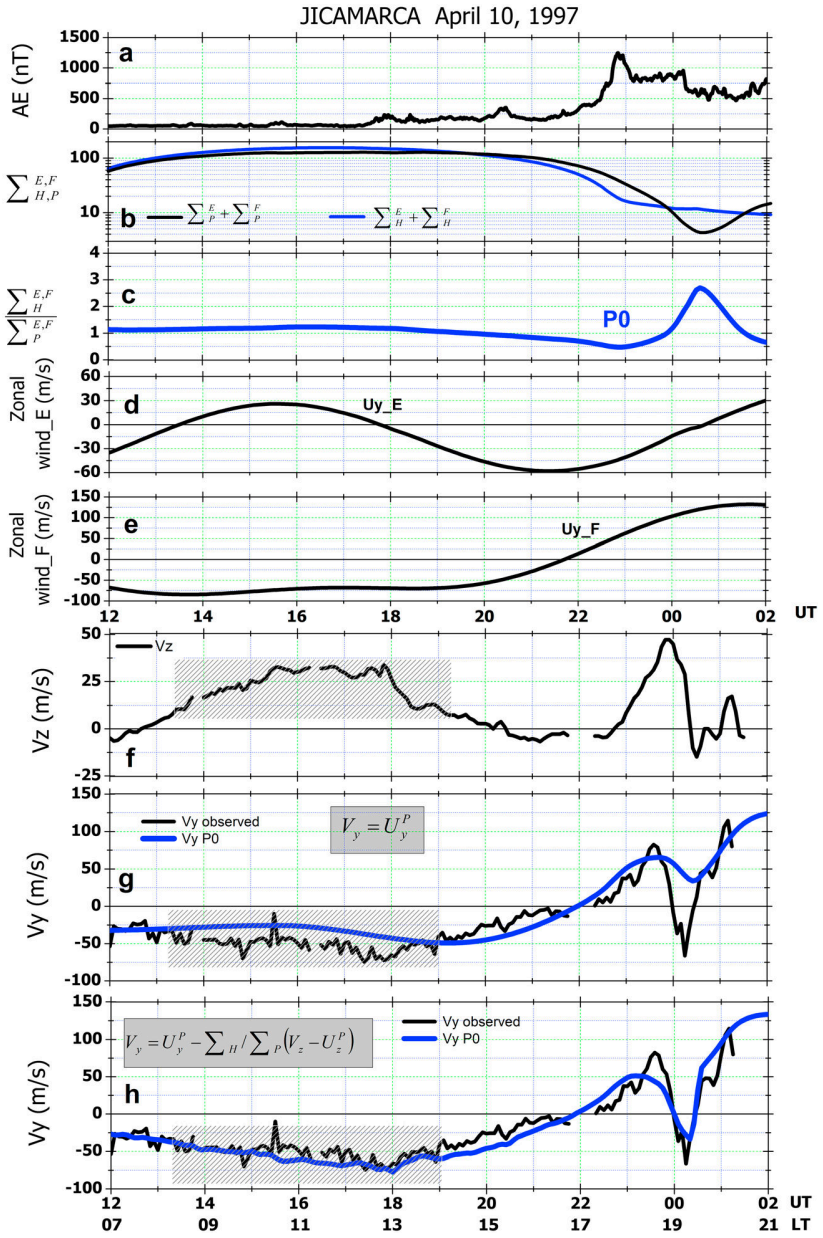

Figure 10. The variations of (a) *AE* index, the (b) *E* and *F* regions integrated Hall and Pedersen conductivities, the (c) ratio $\frac{\sum_H}{\sum_P}$, the regions (d) *E* and (e) *F* zonal wind, the (f) vertical drift V_z, and the (g and h) experimental and calculated zonal drift V_y for different conditions. The shaded area indicates some intervals in which the zonal drifts are discussed in the text.

conductivity decay in comparison with Hall, as it can be clearly seen in Figure 10b. In fact, the modeling has revealed that the eastward prompt penetration electric field makes the low-latitude *F* region ionization to vanish, consequently producing a decrease in the Pedersen conductivity. Another important point that can be noticed in Figure 10 is that between 13 and 19 UT (highlighted by the shaded area in f, g, and h) the observed zonal drift is better represented by the zonal drift calculated by including also the Hall conduction term as can be noted in h, in comparison to g, in which the Hall conduction term was not included. This result is a consequence of the expressive value of the vertical drift V_z (>30 m/s), (Figure 10f) with the ratio $\frac{\sum_H}{\sum_P}$ being close to one in this interval. The model results presented in Figure 10h shows generally good agreement with

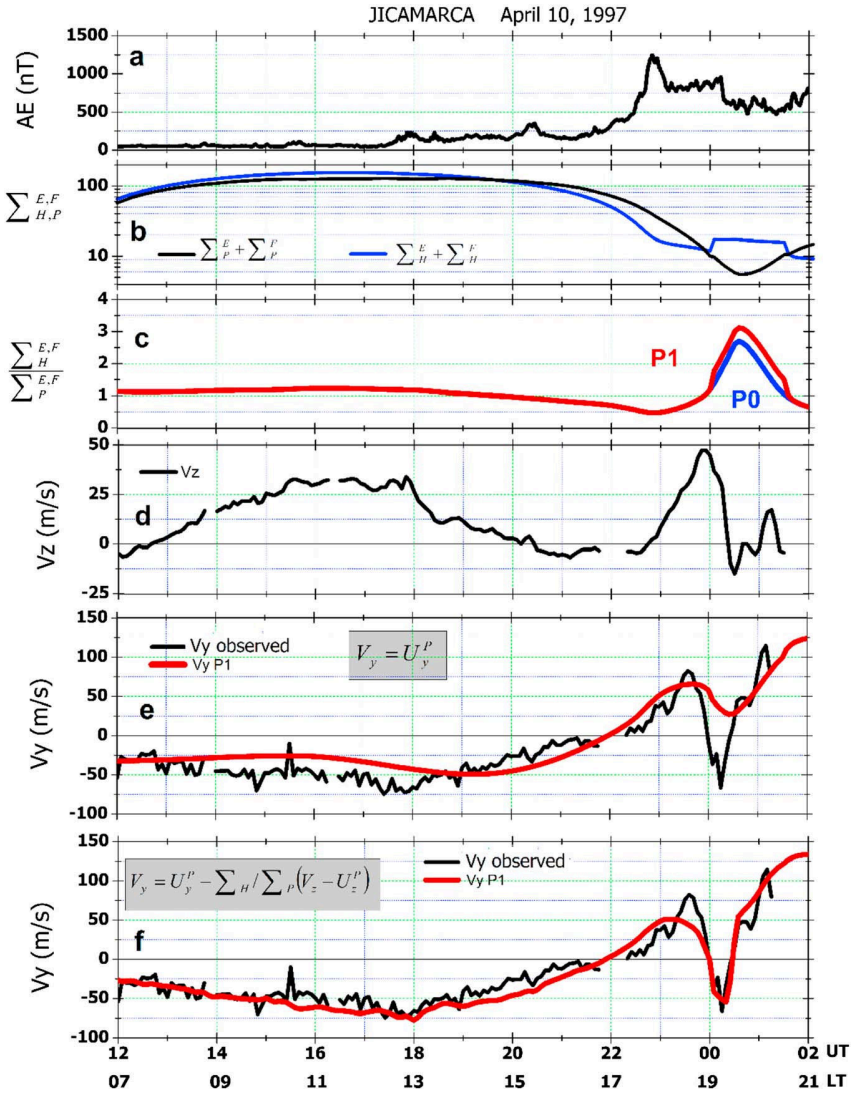

Figure 11. Similar to Figure 10, but here the calculations of the zonal drift was made considering an increase in ionization of the *E* region by the particle precipitation.

observed data. Although the feature of zonal drift reversal to westward near 19 LT is accounted for by the increase in the background conductivity ratio $\frac{\sum_H}{\sum_P}$ at this time (in Figure 10c), we observe a difference of ~ 38 m/s at 0010 UT that is not explained only by this increase alone. With the intention of finding an explanation to this difference, the same methodology used in the previous event was used here, and so an increase in the *E* region conductivity by particle precipitation was included in the calculation.

Similar to Figure 10 but without the plots of zonal winds, Figure 11 shows the zonal drift considering an increase in the ionization of *E* region. When we compare the calculated drift of Figure 11e with the drift of Figure 10g, we note that the particle precipitation had only a small influence in the drift results. Only a difference of ~5 m/s at ~1915 LT could be identified. This is because in the drift calculated using the equation (3), the only parameter that was modified with inclusion of particle precipitation was the Pedersen conductivity, which suffered only little change.

Regarding the results presented in Figure 11f, on the zonal drift reversal to west (near 1910 LT) we note that an increase in the ratio $\frac{\sum_H}{\sum_P}$ due to particle precipitation as shown in Figure 11c (between 19 and 2010LT) was

essential for achieving a better agreement between observed and calculated drifts. To make this possible, it was necessary to increase the ratio $\frac{\sum_H}{\sum_P}$ from ~1.87 to ~2.24, which corresponded to an increase of $\sum_H$ from 11.6 (S/m) to 17.23 (S/m), and the $\sum_P$ from 6.2 (S/m) to 7.6 (S/m). In this case, the electron flux used was less than in the event of June 2008 and varied from 8.6×10^2 el cm^{-2} s^{-1} to 1.9×10^2 el cm^{-2} s^{-1} in the energy range from 2 and 32 keV.

Finally, the results discussed in this section showed that the zonal drift inversion to west has an essential influence of a decrease in the integrated Pedersen conductivity (arising from the *F* region segment of the field line, as seen in Figure 11b probably caused by a prompt penetration zonal electric field (even though a small increase in it due to particle precipitation must have occurred in the *E* layer segment). Additionally, it was shown that if a small increase in the *E* region Hall conductivity was included in the calculation of the zonal drift, a better agreement between the observed and simulated data could be found.

4. Conclusions

The connection between ionospheric vertical and zonal plasma drifts over the Peruvian region, during magnetic storm disturbances was investigated here based on comparisons between the observational data and model results obtained using simulation of the low-latitude ionosphere by the SUPIM-INPE model. The analysis procedure involved quantitative evaluation of field line-integrated physical parameters responsible for driving the zonal plasma drift under quiet and magnetically disturbed conditions and to compare the resulting plasma drifts with their observed variations as measured by the Jicamarca ISR. Simultaneous data of the vertical plasma drift measured by the ISR served as an important control parameter in this analysis. Data from Digisondes in Peru and Brazil were also used to verify the background ionospheric conditions. The study was carried out for two moderate to weak magnetic storm events that occurred during two solar minimum epochs. One of these (that of 24 June 2008) represented the extended deep solar minimum of the recent solar cycle. The other one (that of 10 April 1997) represented a normal solar minimum epoch. The Hall and Pedersen field line-integrated conductivities and the extraionization in the night *E* region that modify their ratio as well as the Pedersen conductivity weighted effect on zonal wind arising from *F* layer density variations were evaluated to examine their impacts on the interrelated oscillations in the vertical and zonal plasma drifts observed under forcing by storm time penetration electric fields. The results obtained during both the solar minimum activity epochs were consistent. However, the quiet daytime zonal drift pattern during the 2008 solar minimum was distinctly different from that of 1997, in that the afternoon eastward reversal of the drift occurred 2 h earlier during the former epoch than during the latter. Some specific conclusions of this study may be summarized as follows:

1. Prompt penetration electric field of eastward polarity associated with the development/initial phase of a storm can cause large vertical plasma drifts in the evening sector of the equatorial ionosphere where the prereversal vertical drift (PRE) can contribute to enhance the vertical drift (depending upon the season). The simultaneous zonal plasma drift suffers large westward increase, in such a way that the two components of the plasma drift tend to appear anti-correlated.
2. Since the anticorrelated drift oscillations in this study were all observed during the beginning of the magnetic storm, the effects of disturbed winds could be totality ignored as an influencing factor in the disturbance zonal drift, and further the calculations considering only the parameter U_y^P clearly showed that the zonal drift fluctuations could not be described only in terms of changes (decrease) in integrated Pedersen conductivity, thus highlighting the important contribution of the parameter that involves the ratio $\frac{\sum_H}{\sum_P}$. Adjustment in this ratio using enhancement in the night time *E* region ionization due to energetic particle precipitation resulted in perfect agreement between the calculated and observed zonal drifts at the time when the vertical and zonal drifts were anti correlated. This is clear evidence that Hall electric field induced by the primary zonal penetration electric field under enhanced *E* layer conductivity due to particle precipitation is an important source of variability in the disturbance zonal drift.
3. Evidence of ionization enhancement contributing to the increase in the ratio $\frac{\sum_H}{\sum_P}$ responsible for the zonal drift fluctuations was inferred from important characteristics of sporadic *E* layers observed in the ionograms over Jicamarca, Fortaleza, and Cachoeria Paulista. More specifically, the Digisonde ionograms over Cachoeira Paulista showed strong E_s layer formed at higher altitudes than generally observed.

4. The zonal drifts for different levels of solar minimum activity showed that during the year 2008 the time of the drift reversal to east in the afternoon was considerably earlier in time (by ~ 2 h) in relation to other period evaluated which suggested that the daytime ionospheric characteristics during the extended solar minimum epoch differed from those of other solar minimum epochs. This aspect will be discussed in a separate study.
5. The zonal and vertical drifts in April 1997 were strongly affected by the action of penetration electric fields. The decrease in integrated Pedersen conductivity was very important but not sufficient to explain the fluctuations in zonal drift. It was found that if an increase in ionization of the *E* region was considered, a better result of calculated zonal drift could be found.
6. The zonal drift calculated in April 1997, which also corresponds to a solar minimum period, showed that the model wind used in the calculation was consistent with the observed zonal drift and therefore represented realistic wind, in contrast to June 2008 for which the HWM93 model wind was not representative of the real wind.

Finally, we may point out that the zonal plasma drift fluctuations due to penetration electric field have received only very limited attention in the literature, whereas this question poses significant challenges for the development of models on predicting plasma bubble irregularities and scintillation occurrences at specific location along the equatorial region. In this study we have shown through quantitative evaluations that Hall conduction effect, besides the conductivity weighted zonal winds, under the influence of disturbance electric field, are important parameters to be considered in the development of prediction models.

Acknowledgments
A.M. Santos acknowledges the Conselho Nacional de Desenvolvimento Científico e Tecnológico - CNPq for the financial support under grants 150403/2015 and 160088/2011-9. The *SYM-H AE* and IMF data were obtained from the website http://omniweb.gsfc.nasa.gov/form/omni_min.html. The authors gratefully acknowledge the Jicamarca staff for providing drifts data from IRS. The Jicamarca Radio Observatory is a facility of the Instituto Geofisico del Peru operated with support from the NSF AGS-0905448 through Cornell University. M.A.A. acknowledges the support received from the Coordenação de Aperfeiçoamento de Pessoal de Nível Superior (Capes) for a senior visiting professorship at ITA/DCTA.

References

Abdu, M. A. (1997), Major phenomena of the equatorial ionosphere-thermosphere system under disturbed conditions, *J. Atmos. Sol.-Terr. Phys.*, *59*, 1505–1519, doi:10.1016/S1364-6826(96)00152-6.

Abdu, M. A. I. S. Batista, L. R. Piazza, and O. Massambani (1981), Magnetic storm associated enhanced particle precipitation in the South Atlantic Anomaly evidence from VLF phase measurements, *J. Geophys. Res.*, *86*, 7533–7542, doi:10.1029/JA086iA09p07533.

Abdu, M. A. I. S. Batista, G. O. Walker, J. H. A. Sobral, N. B. Trivedi, and E. R. De Paula (1995), Equatorial ionospheric electric fields during magnetospheric disturbances: Local time/longitude dependences from recent EITS campaigns, *J. Atmos. Sol. Terr. Phys.*, *57*(10), 1065–1083, doi:10.1016/0021-9169(94)00123-6.

Abdu, M. A. P. T. Jayachandran, J. MacDougall, J. F. Cecile, and J. H. A. Sobral (1998), Equatorial *F* zonal plasma irregularity drifts under magnetospheric disturbances, *Geophys. Res. Lett.*, *25*(22), 4137–4140, doi:10.1029/1998GL900117.

Abdu, M. A., I. S. Batista, H. Takahashi, J. MacDougall, J. H. Sobral, A. F. Medeiros, and N. B. Trivedi (2003), Magnetospheric disturbance induced equatorial plasma bubble development and dynamics: A case study in Brazilian sector, *J. Geophys. Res.*, *108*(A12), 1449, doi:10.1029/2002JA009721.

Abdu, M. A., I. S. Batista, A. J. Carrasco, and C. G. M. Brum (2005), South Atlantic magnetic anomaly ionization: a review and a new focus on electrodynamic effects in the equatorial ionosphere, *J. Atmos. Sol.-Terr. Phys.*, *67*, 1643–1657.

Abdu, M. A., J. R. de Souza, J. H. A. Sobral, and I. S. Batista (2006), Magnetic storm associated disturbance dynamo effects in the low and equatorial latitude ionosphere, in *Recurrent Magnetic Storms: Corotating Solar Wind Streams*, *Geophys. Monogr. Ser.*, vol. 167, edited by B. Tsurutani et al., pp. 283–304, AGU, Washington, D. C., doi:10.1029/167GM22.

Abdu, M. A. T. Maruyama, I. S. Batista, S. Saito, and A. M. Nakamura (2007), Ionospheric responses to the October 2003 superstorm: Longitude/local time effects over equatorial low and middle latitudes, *J. Geophys. Res.*, *112*, A10306, doi:10.1029/2006JA012228.

Abdu, M. A. E. A. Kherani, I. S. Batista, and J. H. A. Sobral (2009), Equatorial evening prereversal vertical drift and spread *F* suppression by disturbance penetration electric fields, *Geophys. Res. Lett.*, *36*, L19103, doi:10.1029/2009GL039919.

Abdu, M. A. I. S. Batista, F. Bertoni, B. W. Reinisch, E. A. Kherani, and J. H. A. Sobral (2012), Equatorial ionosphere responses to two magnetic storms of moderate intensity from conjugate point observations in Brazil, *J. Geophys. Res.*, *117*, A05321, doi:10.1029/2011JA017174.

Abdu, M. A. J. R. Souza, I. S. Batista, B. G. Fejer, and J. H. A. Sobral (2013), Sporadic E layer development and disruption at low latitudes by prompt penetration electric fields during magnetic storms, *J. Geophys. Res. Space Physics*, *118*, 2639–2647, doi:10.1002/jgra.50271.

Abdu, M. A. J. R. de Souza, I. S. Batista, A. M. Santos, J. H. A. Sobral, R. G. Rastogi, and H. Chandra (2014), The role of electric fields in sporadic *E* layer formation over low latitudes under quiet and magnetic storm conditions, *J. Atmos. Sol.-Terr., Phys. 115–116*, 95–105, doi:10.1016/j.jastp.2013.12.003.

Bailey, G. J. and N. Balan (1996), Some modelling studies of the equatorial ionosphere using the Sheffield University Plasmasphere Ionosphere Model, *Adv. Space Res.*, *18*(6), 59–68, doi:10.1016/0273-1177(95)00901-9.

Bailey, G. J. R. Sellek, and Y. Rippeth (1993), A modeling study of the equatorial topside ionosphere, *Ann. Geophys.*, *11*(4), 263–272.

Bailey, G. J. N. Balan, and Y. Z. Su (1997), The Sheffield University Ionosphere Plasmasphere Model—A review, *J. Atmos. Sol. Terr. Phys.*, *59*(13), 1541–1552, doi:10.1016/S1364-6826(96)00155-1.

Batista, I. S. and M. A. Abdu (1977), Magnetic storm associated delayed sporadic *E* enhancements in the Brazilian Geomagnetic Anomaly, *J. Geophys. Res.*, *82*, 4777–4783, doi:10.1029/JA082i029p04777.

Batista, I. S. E. R. de Paula, M. A. Abdu, N. B. Trivedi, and M. E. Greenspan (1991), Ionospheric effects of the March 13, 1989, magnetic storm at low and equatorial latitudes, *J. Geophys. Res.*, *96*(A8), 13,943–13,952, doi:10.1029/91JA01263.

Batista, I. S. M. A. Abdu, J. R. Souza, F. Bertoni, M. T. Matsuoka, P. O. Camargo, and G. J. Bailey (2006), Unusual early morning development of the equatorial anomaly in the Brazilian sector during the Halloween magnetic storm, *J. Geophys. Res.*, *111*, A05307, doi:10.1029/2005JA011428.

Biondi, M. A. S. Y. Sazykin, B. G. Fejer, J. W. Meriwether, and C. G. Fesen (1999), Equatorial and low-latitude thermospheric winds: Measured quiet time variations with season and solar flux from 1980 to 1990, *J. Geophys. Res.*, *104*, 17,091–17,106, doi:10.1029/1999JA900174.

Blanc, M. and A. D. Richmond (1890), The ionospheric disturbance dynamo, *J. Geophys. Res.*, *85*, 1669–1699, doi:10.1029/JA085iA04p01669.
Del Pozo, C. F. J. K. Hargreaves, and A. D. Aylward (1997), Ion composition and effective ion recombination rate in the nighttime auroral lower ionosphere, *J. Atmos. Sol.-Terr. Phys.*, *59*(15), 1919–1943, doi:10.1016/S1364-6826(97)00033-3.
Eccles, J. V. (1998), A simple model of low latitude electric fields, *J. Geophys. Res.*, *103*, 26,699–26,708, doi:10.1029/98JA02657.
Fejer, B. G., and J. T. Emmert (2003), Low latitude ionospheric disturbance electric field effects during the recovery phase of the October 19–21, 1998, magnetic storm, *J. Geophys. Res.*, *108*(A12), 1454, doi:10.1029/2003JA010190.
Fejer, B. G. D. T. Farley, C. A. Gonzales, R. F. Woodman, and C. Calderon (1981), *F* region east-west drifts at Jicamarca, *J. Geophys. Res.*, *86*, 215–218, doi:10.1029/JA086iA01p00215.
Fejer, B. G. E. Kudeki, and D. T. Farley (1985), Equatorial *F* region zonal plasma drifts, *J. Geophys. Res.*, *90*, 12,249–12,255, doi:10.1029/JA090iA12p1224.
Fejer, B. G. E. R. de Paula, S. A. González, and R. F. Woodman (1991), Average vertical and zonal *F*-region plasma drifts over Jicamarca, *J. Geophys. Res.*, *96*(A8), 13,901–13,906, doi:10.1029/91JA01171.
Fejer, B. G. J. De Souza, A. S. Santos, and A. E. C. Pereira (2005), Climatology of *F* region zonal plasma drifts over Jicamarca, *J. Geophys. Res.*, *110*, A12310, doi:10.1029/2005JA011324.
Gonzalez, W. D. J. A. Joselyn, Y. Kamide, H. W. Kroehl, G. Rostoker, B. T. Tsurutani, and V. M. Vasyliunas (1994), What is a magnetic storm? *J. Geophys. Res.*, *99*(A4), 5771–5792, doi:10.1029/93JA02867.
Haerendel, G. J. V. Eccles, and S. Çakir (1992), Theory for modeling the equatorial evening ionosphere and the origin of shear in the horizontal plasma flow, *J. Geophys. Res.*, *97*(A2), 1209–1223, doi:10.1029/91JA02226.
Hedin, A. E. et al. (1996), Empirical wind model for the upper, middle and lower atmosphere, *J. Atmos. Terr. Phys.*, *58*, 1421–1447, doi:10.1016/0021-9169(95)00122-0.
Kelley, M. C. B. G. Fejer, and C. A. Gonzales (1979), An explanation for anomalous equatorial ionospheric electric fields associated with a northward turning of the interplanetary magnetic field, *Geophys. Res. Lett.*, *6*(4), 301–304, doi:10.1029/GL006i004p00301.
Kikuchi, T. K. K. Hashimoto, and K. Nozaki (2008), Penetration of magnetospheric electric fields to the equator during a geomagnetic storm, *J. Geophys. Res.*, *113*, A06214, doi:10.1029/2007JA012628.
Liu, L. J. Yang, H. Le, Y. Chen, W. Wan, and C.-C. Lee (2012), Comparative study of the equatorial ionosphere over Jicamarca during recent two solar minima, *J. Geophys. Res.*, *117*, A01315, doi:10.1029/2011JA017215.
Mann, L. G. S. D. Bloom, and H. I. West Jr. (1963), The electron spectrum from 90 to 1200 keV as observed on Discoverer satellites 29 and 31, *Space Res.*, 447–482.
Mannucci, A. J. B. T. Tsurutani, B. A. Iijima, A. Komjathy, A. Saito, W. D. Gonzalez, F. L. Guarnieri, J. U. Kozyra, and R. Skoug (2005), Dayside global ionospheric response to the major interplanetary events of October 29–30, 2003 "Halloween Storms", *Geophys. Res. Lett.*, *32*, L12S02, doi:10.1029/2004GL021467.
Mathews, J. D. (1998), Sporadic *E*: Current views and recent progress, *J. Atmos. Sol.-Terr. Phys.*, *60*(4), 413–435, doi:10.1016/S1364-6826(97)00043-6.
McDiarmid, I. B. D. C. Rose, and E. Budzinski (1961), Direct measurement of charged particles associated with auroral zone radio absortion, *Can. J. Phys.*, *39*, 1888–1900.
Picone, J. M., Hedin, A. E., Drob, D. P., and Aikin, A. C. (2002), NRLMSISE-00 empirical model of the atmosphere: Statistical comparisons and scientific issues, *J. Geophys. Res.*, *107*(A12), 1468, doi:10.1029/2002JA009430.
Rees, M. H. (1963), Auroral ionization and excitation by incident energetic electrons, *Planet. Space Sci.*, *11*, 1209–1218, doi:10.1016/0032-0633(63)90252-6.
Rees, M. H. (1989), *Physics and Chemistry of the Upper Atmosphere*, pp. 289, Cambridge Univ. Press, Cambridge, U. K.
Richmond, A. D. and G. Lu (2000), Upper atmospheric effects of magnetic storms: A brief tutorial, *J. Atmos. Sol.-Terr. Phys.*, *62*, 1115–1127, doi:10.1016/S1364-6826(00)00094-8.
Santos, A. M. M. A. Abdu, J. H. A. Sobral, D. Koga, P. A. B. Nogueira, and C. M. N. Candido (2012), Strong longitudinal difference in ionospheric responses over Fortaleza (Brazil) and Jicamarca (Peru) during the January 2005 magnetic storm, dominated by northward IMF, *J. Geophys. Res.*, *117*, A08333, doi:10.1029/2012JA017604.
Sastri, J. H. (1988), Equatorial electric fields of ionospheric disturbance dynamo origin, *Ann. Geophys.*, *6*, 635–642.
Sastri, J. H. J. V. S. Visweswara Rao, and K. B. Ramesh (1993), Penetration of polar electric field to the nightside dip equator at times of geomagnetic sudden commencements, *J. Geophys. Res.*, *98*(A10), 17,517–17,523, doi:10.1029/93JA00418.
Scherliess, L. A. and B. G. Fejer (1999), Radar and satellite global equatorial *F* region vertical drift model, *J. Geophys. Res.*, *104*(A4), 6829–6842.
Scherliess, L. and B. G. Fejer (1997), Storm time dependence of equatorial disturbance dynamo zonal electric fields, *J. Geophys. Res.*, *102*(A11), 24,037–24,046, doi:10.1029/97JA02165.
Sobral, J. H. A. M. A. Abdu, W. D. González, B. T. Tsurutani, I. S. Batista, and A. L. Clua de González (1997), Effects of intense storms and substorms on the equatorial ionosphere/thermosphere system in the American sector from ground-based and satellite data, *J. Geophys. Res.*, *102*(A7), 14,305–14,313, doi:10.1029/97JA00576.
Sobral, J. H. A. M. A. Abdu, C. S. Yamashita, W. D. Gonzalez, A. C. de Gonzalez, I. S. Batista, C. J. Zamlutti, and B. T. Tsurutani (2001), Responses of the low-latitude ionosphere to very intense geomagnetic storms, *J. Atmos. Sol.-Terr. Phys.*, *63*(9), 965–974, doi:10.1016/S1364-6826(00)00197-8.
Tobiska, W. K. T. Woods, F. Eparvierb, R. Viereckc, L. Floydd, D. Bouwere, G. Rottmanb, and O. R. White (2000), The SOLAR2000 empirical solar irradiance model and forecast tool, *J. Atmos. Sol.-Terr. Phys.*, *62*, 1233–1250, doi:10.1016/S1364-6826(00)00070-5.
Tsurutani, B. T. et al. (2008), Prompt penetration electric fields (PPEFs) and their ionospheric effects during the great magnetic storm of October 30–31, 2003, *J. Geophys. Res.*, *113*, A05311, doi:10.1029/2007JA012879.
Whitehead, J. (1970), Production and prediction of sporadic *E*, *Rev. Geophys. Space Phys.*, *8*(1), 65–144, doi:10.1029/RG008i001p00065.
Woodman, R. F. (1972), East-west ionospheric drifts at the magnetic equator, *Space Res.*, *12*, 969–974.